Spectral Ghost Imaging for Ultrafast Spectroscopy

Shir Rabi, Sara Meir, Raphi Dror, Hamootal Duadi, Francesco Baldini, Francesco Chiavaioli, and Moti Fridman

***Abstract*—We experimentally demonstrate ghost imaging in the frequency domain based on frequency speckle patterns as references. Our method is suitable for measuring the spectrum of ultrafast signals with high repetition rates. We study the reconstruction resolution as a function of the signal periodicity and found the maximal signal periodicity which can be reconstructed. We also study the reconstruction resolution as a function of the speckle size and show that the speckle size determines the quality of the ghost image. Finally, we perform numerical and analytical calculations which agree with our experimental measured results. Our method is simple, broadband, and utilizes a low cost bucket detector for ultrafast spectral measurements.**

***Index Terms*—Ghost imaging, spectroscopy, ultrafast spectroscopy.**

I. Introduction

ULTRAFAST spectrometers provide the ability to observe the spectral components of physical, biological and chemical phenomena in high temporal resolution. Some known methods are frequency resolved optical gating (FROG) [1], spectral phase interferometry for direct electric field reconstruction (SPIDER) [2] and pump probe spectroscopy [3], [4]. All of these methods require complex non-linear scheme and have a limited spectral bandwidth. A simpler and broader technique is time stretch, also known as dispersive Fourier transform [5], [6], which is based on dispersive broadening of pulses in optical fibers. However, this method is not suitable for signals with high repetition rates, due to overlapping between adjacent signals. In order to overcome this limitation, we developed an ultrafast spectrometer based on spectral ghost imaging which can obtain high resolution spectrum with about 150 measurements.

In ghost imaging, we illuminate an object with a reference beam, and then detect it by a single pixel bucket detector [7]. By correlating the detection with the known reference beam, we reconstruct a high resolution image of the object. Ghost imaging was demonstrated originally in the spatial domain, in both quantum [8], [9] and classical [10] approaches. With the advancement of research on space-time duality [11], an extension to the time domain was suggested [12]. Recently, ghost imaging in the spectral domain was also studied, both in quantum [13] and classical [14], [15] approaches. We implement spectral ghost imaging in time stretch systems to improve the spectral resolution for signals with high repetition rates. Our method is simple, broadband, independent of the time stretch fiber length, and utilizes a low cost bucket detector. It can be implemented for investigating the spectrum in ultrafast processes [16], [17], or for researching light-matter interactions [18], [19]. It can also be implemented for mapping the spectrum of non-linear fiber processes with a high repetition rate pump [20]–[23].

In order to generate the speckle field, we take advantages of a recently-explored kind of fiber grating, called pseudo-random long-period fiber grating [24], [25]. This fiber grating can generate different types of spectral speckle fields and the speckle field is shifted by inducing stresses on the grating via piezo actuators. However, in order to analyze our method with a flexible system, with different speckle fields and with different shifts, we resort to a slower pulse-shaper scheme.

II. Analytical Derivation

We start with analytically deriving the ghost imaging procedure in the frequency domain. Let our signal be $G(\omega)$ and our speckle pattern be $S(\omega)$. In each measurement, we shift the speckle pattern by ν. Imposing the shifted speckle on the signal leads to: $G(\omega)S(\omega-\nu)$, and integrating it over the spectrum due to the low resolution of our detector gives:

$$B(\nu) = \int G(\omega)S(\omega-\nu)\,d\omega. \tag{1}$$

This measurement is identical to a bucket detector, in which we are summing over all the wavelengths. To get the ghost image, we multiply $B(\nu)$ by the speckle pattern $S(\omega'-\nu)$ and integrate over all the possible ν leading to:

$$GI(\omega') = \int B(\nu)S(\omega'-\nu)\,d\nu. \tag{2}$$

We place (1) into (2), and rearrange the integration order:

$$\begin{aligned} GI(\omega') &= \int G(\omega)S(\omega-\nu)\,d\omega S(\omega'-\nu)\,d\nu \\ &= \int G(\omega)\int S(\omega-\nu)S(\omega'-\nu)\,d\nu\,d\omega, \end{aligned} \tag{3}$$

and by placing $\xi = \omega - \nu$ we get:

$$\int S(\omega-\nu)S(\omega'-\nu)d\nu = \int S(\xi)S(\xi+(\omega'-\omega))d\xi. \tag{4}$$

Manuscript received December 8, 2021; accepted December 22, 2021. Date of publication December 31, 2021; date of current version January 11, 2022. This work was supported by the Israeli Science Foundation under Grant 2096/20. *(Corresponding author: Shir Rabi.)*

Shir Rabi, Sara Meir, Hamootal Duadi, and Moti Fridman are with the Faculty of Engineering and the Institute of Nanotechnology and Advanced Materials, Bar-Ilan University, Ramat Gan 5290002, Israel (e-mail: shirbrabi@gmail.com; sarameir694@gmail.com; hamootal@gmail.com; moti43@gmail.com).

Raphi Dror is with the Applied Physics Department, Soreq NRC, Yavne, NA 8180000, Israel (e-mail: raphi.dror@gmail.com).

Francesco Baldini and Francesco Chiavaioli are with the National Research Council of Italy, Institute of Applied Physics "Nello Carrara", 50019 Sesto Fiorentino, Italy (e-mail: f.baldini@ifac.cnr.it; f.chiavaioli@ifac.cnr.it).

Digital Object Identifier 10.1109/JPHOT.2021.3138689

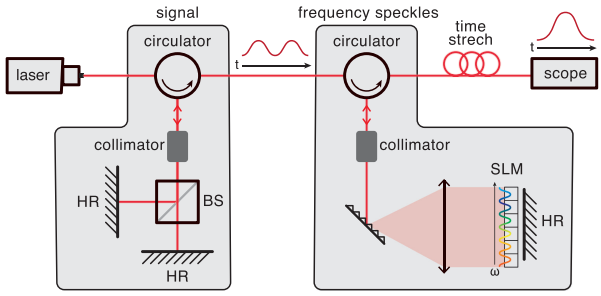

Fig. 1. Experimental setup for ghost imaging. We generate a double pulse signal by splitting a laser pulse into two. Next, we send the signal through a 2f system to a spatial light modulator, thus imposing frequency speckles on it. Finally, we detect the signal with a low resolution time stretch system. BS: beam splitter. SLM: spatial light modulator. DCF: dispersion compensating fiber.

The auto-correlation of a speckle is proportional to [26], [27] $sinc^2((\omega-\omega')/\Delta\omega)$, where $\Delta\omega$ is the size of each speckle. When the speckle size is small, this can be approximated to $\delta(\omega-\omega')$ [27], [28], hence:

$$GI(\omega') = \int G(\omega)\delta(\omega-\omega')\,d\omega = G(\omega') \tag{5}$$

Thus, we reconstruct the original signal. When the speckle size is larger, we cannot approximate to a delta function, so, the resolution of the ghost image is determined by the speckle size, $\Delta\omega$.

In our method, we aim to generate the speckle field via pseudo-random long-period fiber grating and to shift the output by inducing stresses with piezo actuators. Therefore, we are shifting the speckle field between each measurement instead of choosing a new random speckle field. This may lead to introducing artifacts to the image or smearing some details of the signal. However, as long as the auto-correlation of the speckle field has a sharp peak around zero without significant side-lobs, and as long as the features of the signal are larger than the peak of the auto-correlation, our method will result in a high resolution spectral image of the input signal spectrum.

III. Experimental Setup and Results

We experimentally demonstrate spectral ghost imaging with our system, which is schematically shown in Fig. 1. We start with a laser pulse with a central wavelength of $1531 \pm 5\ nm$ and a repetition rate of 100 MHz. We split it into two pulses separated by 6 ps and increase the separation up to 39 ps. Thus, we obtain fringes in the frequency domain with a periodicity between 0.2 nm and 1.3 nm.

Next, we impose the frequency speckles on our signal. To generate the frequency speckles, we diffract the beam by a $600 lines/mm$ grating, sending it through a 2f system of 1 m focal length, towards a spatial light modulator (Jenoptik, SLM-S640). Each 0.16 nm spectral bandwidth encounters a different pixel on the SLM. By controlling the voltage of each pixel individually, we tailor a random amplitude pattern on our signal, according to the spectral response of our pseudo-random long-period fiber grating. This random pattern serves as the frequency speckle pattern. We measured a representative speckle pattern with an optical spectrum analyzer (OSA) and show it in Fig. 2(a).

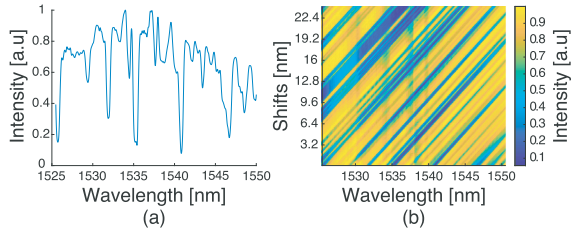

Fig. 2. Speckle reference for our spectral ghost imaging. The frequency speckle pattern is shifted by 0.16 nm between measurements. (a) A single measurement of a frequency speckle pattern. (b) One hundred and fifty shifted frequency speckles.

We reflect the output from the SLM with a high-reflection mirror through the 2f system again. Next, we pass it through a 400 m dispersion compensating fiber (DCF-38, Thorlabs) to impose dispersion for the time to frequency mapping. Note that 400 m leads to a spectral resolution which is not enough for measuring the spectral fringes of the input signal. Thus, our low resolution measurement serves as a temporal bucket detector.

In order to obtain the ghost image and reconstruct our signal, we take 150 measurements and in each one, we shift the phase mask by 0.16 nm. We measure all the 150 shifted speckle patterns with the OSA, shown in Fig. 2(b). In addition, we measure the output spectrum of the signal including the frequency speckle with the low spectral resolution time-stretch system. Each measurement has a Gaussian shape with a different height. We record the maximum of each Gaussian and multiply it by its frequency speckle pattern. Finally, we sum over all these measurements to reconstruct the input signal spectrum with a high resolution. Therefore, we obtain a high resolution spectral measurement every 1.5 μs.

Representative input signals with spectral periodicity of 0.2 nm and 0.7 nm (orange dashed curves) and their reconstructed ghost images (blue solid curves) are shown in Fig. 3(a) and (b), respectively. The reconstructed ghost image of a signal with 0.7 nm spectral periodicity has high visibility with a signal-to-noise ratio of 5, while the signal with 0.2 nm spectral periodicity leads to lower visibility with a signal-to-noise ratio of less than 2. This is due to the 0.5 nm size of our frequency speckle, which determines the resolution of the reconstruction. We repeated these measurements for other random speckle patterns and all of them retrieved the correct spectral oscillations of the input signal. The retrieved spectral oscillations have some deviations which lead to the out-of-phase oscillations at wavelengths above 1534 nm.

Time-stretch systems can measure the spectrum of each pulse separately and identify fast spectral dynamics by comparing the spectrum of adjacent pulses. However, time-stretch system does not have the accuracy or the dynamic range of slow spectrometers which average over large number of pulses. Therefore, the measured spectrum, shown in Fig. 3(b), has lower oscillations amplitude of about half than the oscillations measured by the slow optical spectrum analyzer. Nevertheless, the measured oscillations frequency is accurate and the relative intensities of the different peaks are also accurate. We note that our system cannot measure the spectrum of each pulse, since it still uses about 150 measurements, but this is still much shorter time

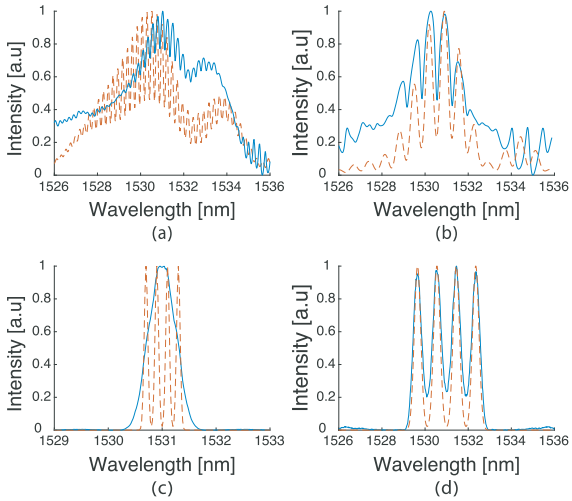

Fig. 3. Comparison between signals and their ghost images. Subplots (a) and (b) are the experimental results for signals with spectral periodicity of 0.2 nm and 0.7 nm, respectively. The orange dashed curve denotes the signal, and the blue curves denote their ghost images. The measured ghost image of the signal with a spectral periodicity of 0.2 nm has a lower visibility than the measured ghost image of 0.7 nm. Subplots (c) and (d) are representative calculated results for signals with spectral periodicities of 0.2 nm and 0.7 nm, respectively. The calculated ghost images of the signal with a spectral periodicity of 0.2 nm has lower visibility than the calculated ghost image of 0.7 nm, in agreement with the measured results.

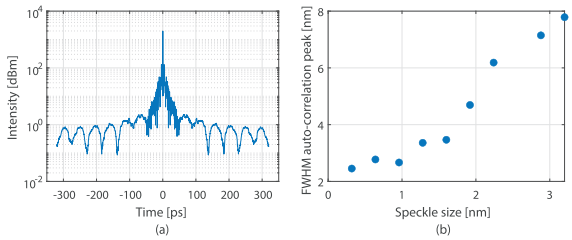

Fig. 4. Analysis of the spectral speckle field. (a) Fourier transform of the spectral speckle field. (b) Full-width half maximum of the auto-correlation peak of speckle patterns as a function of the speckle sizes in the pattern.

scales compared to the long averaging time of optical spectrum analyzers.

We analyzed the spectral speckle field and verified that its properties are suitable for ghost imaging. We performed Fourier transform of the speckle pattern and present it in Fig. 4(a). Since the speckle pattern is in the frequency-domain, its Fourier transform is in the time-domain, and the zero order is high since we do not measure the phase. We observed a relative smooth curve without significant features up to 50 ps with an intensity reduction of two orders of magnitudes. These results indicate that the pattern is indeed random and has no self-similar spectral features. At longer times, above 50 ps, there are some features, however, their relative intensities are much lower and therefore, they have no impact on our system. We also evaluated the auto-correlation of the speckle field and studied the width of the main peak. The width of the main peak determines the spectral resolution of our system. We present the full-width half maximum (FWHM) of the peak of the auto-correlation as a function of the speckle sizes in the pattern in Fig. 4(b). As expected, we obtained an increasing trend. We attribute the

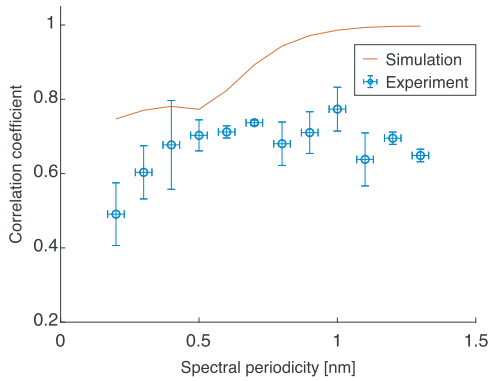

Fig. 5. Correlation between our reconstructed ghost images and the input signal as a function of the spectral periodicity. The orange curve denotes the calculated correlation and the blue circles denote the experimental results. As we increase the spectral periodicity, the resolution of the ghost image improves.

deviations from a linear curve to the finite size of our speckle pattern.

We performed numerical calculations to verify our results. We simulated the analytic derivation in (2) with signals composed of four peaks. We randomized a speckle pattern, and calculated the ghost image of the signal, for signals with different spectral periodicities. Representative results for signals with spectral periodicities of 0.2 nm and 0.7 nm are shown in Fig. 3(c) and (d), respectively. The calculated reconstruction of a signal with 0.7 nm spectral periodicity has higher visibility than the calculated reconstruction of the signal with 0.2 nm spectral periodicity. These calculated results agree with the measured ones.

In order to investigate the resolution limit of our system, we conducted twelve experiments, where in each experiment we changed the spectral periodicity of the signal. We measured signals with spectral periodicities of: $0.2, 0.3, 0.4, 0.5, 0.6, 0.7, 0.8, 0.9, 1, 1.2$ and $1.3\ nm$. To quantify the quality of the reconstructed ghost images, we evaluated the correlation between the input signals and the ghost images for each spectral periodicity. We present the results by the circles in Fig. 5. As evident, the correlation coefficient grows as we increase the spectral periodicity, until reaching a correlation coefficient of 0.7 at 0.5 nm. This verifies that our spectral resolution is 0.5 nm in agreement with the speckle size.

To quantify the quality of the signal reconstruction numerically, we calculated the correlation coefficient between the ghost image and the signal. We repeated this calculation with 50 different frequency speckle patterns, averaging the results. As we increase the spectral periodicity, the correlation coefficient grows. These results are presented by the orange curve in Fig. 5. We attribute the discrepancy between the experimental measurements and the calculated results to deviations in the speckle size. During the experiment, the speckle size is not 0.5 nm along the entire speckle field. Hence, it increases the correlation for spectral periodicities lower than 0.5 nm. Nevertheless, the calculated correlation increases as we increase the spectral periodicity, similar to the experimental results but for larger spectral periodicities.

Next, we investigate the influence of the speckle size on the reconstruction quality. We examined the resolution of the reconstruction of two signals with spectral periodicities of

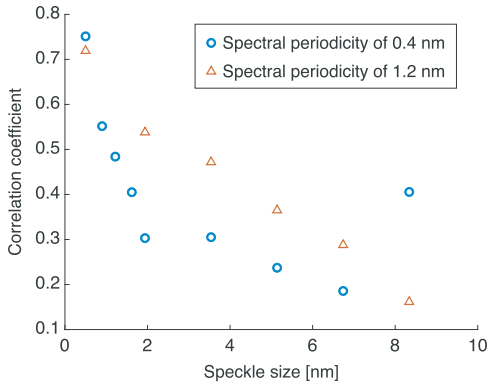

Fig. 6. Correlation between our ghost image reconstruction and the original measured spectral signal for spectral periodicities of 0.4 and 1.2 nm as a function of the speckle size. As we increase the size of the speckle, the quality of the ghost image decreases.

0.4 nm and 1.2 nm. In each measurement, we increased the size of our speckles and calculated the correlation coefficient between the ghost image and the input signal. The results are shown in Fig. 6. As evident, for both cases the correlation coefficient decreases as we increase the speckle size. However, for a spectral periodicity of 0.4 nm (blue circle), the correlation decreases sharply as we increased the speckle size to 2 nm. While, for spectral periodicity of 1.2 nm, the correlation decreases moderately as we increase the speckle size. These results confirm that the speckle size $\Delta\omega$ determines the ghost image resolution according to our analytic derivation. Note that as we changed the size of the speckles, we still shifted them by 0.16 nm between measurements.

IV. Conclusion

We demonstrated that our system can measure the spectrum of high repetition rate pulses, such as short cavities ultrafast lasers. Our method, transmits the input signal through a pseudo-random long-period fiber grating and measure the total transmission. Changing the grating parameters by either short pump pulses or piezo actuators, shifts the speckle field leading to the reconstruction of the high resolution spectral measurement with a sampling rate of 1/100 of that of the input signal. By averaging over larger number of measurements, we can improve the resolution and signal-to-noise ratio, on the expanse of the sampling rate.

To conclude, we developed a spectroscopy technique based on spectral ghost imaging with a reference of a frequency speckle pattern. We studied the reconstructed ghost image resolution as a function of the signal periodicity and the speckle resolution. We demonstrated reconstructions of signals with 0.5 nm spectral resolution. Our method is simple, low cost, robust, and can be implemented for high resolution spectroscopy of signals with high repetition rates.

References

[1] D. J. Kane and R. Trebino, "Characterization of arbitrary femtosecond pulses using frequency-resolved optical gating," *IEEE J. Quantum Electron.*, vol. 29, no. 2, pp. 571–579, Feb. 1993.

[2] C. Iaconis and I. A. Walmsley, "Spectral phase interferometry for direct electric-field reconstruction of ultrashort optical pulses," *Opt. Lett.*, vol. 23, no. 10, pp. 792–794, 1998.

[3] T. Ye, D. Fu, and W. S. Warren, "Nonlinear absorption microscopy," *Photochemistry Photobiol.*, vol. 85, no. 3, pp. 631–645, 2009.

[4] A. H. Zewail, "Laser femtochemistry," *Science*, vol. 242, no. 4886, pp. 1645–1653, 1988.

[5] A. Mahjoubfar, D. V. Churkin, S. Barland, N. Broderick, S. K. Turitsyn, and B. Jalali, "Time stretch and its applications," *Nature Photon.*, vol. 11, no. 6, pp. 341–351, 2017.

[6] K. Goda and B. Jalali, "Dispersive Fourier transformation for fast continuous single-shot measurements," *Nature Photon.*, vol. 7, no. 2, pp. 102–112, 2013.

[7] A. Gatti, M. Bache, D. Magatti, E. Brambilla, F. Ferri, and L. Lugiato, "Coherent imaging with pseudo-thermal incoherent light," *J. Modern Opt.*, vol. 53, no. 5-6, pp. 739–760, 2006.

[8] D. Strekalov, A. Sergienko, D. Klyshko, and Y. Shih, "Observation of two-photon "Ghost" interference and diffraction," *Phys. Rev. Lett.*, vol. 74, no. 18, 1995, Art. no. 3600.

[9] T. B. Pittman, Y. Shih, D. Strekalov, and A. V. Sergienko, "Optical imaging by means of two-photon quantum entanglement," *Phys. Rev. A*, vol. 52, no. 5, 1995, Art. no. R3429.

[10] R. S. Bennink, S. J. Bentley, R. W. Boyd, and J. C. Howell, "Quantum and classical coincidence imaging," *Phys. Rev. Lett.*, vol. 92, no. 3, 2004, Art. no. 033601.

[11] B. H. Kolner, "Space-time duality and the theory of temporal imaging," *IEEE J. Quantum Electron.*, vol. 30, no. 8, pp. 1951–1963, Aug. 1994.

[12] P. Ryczkowski, M. Barbier, A. T. Friberg, J. M. Dudley, and G. Genty, "Ghost imaging in the time domain," *Nature Photon.*, vol. 10, no. 3, pp. 167–170, 2016.

[13] G. Scarcelli, A. Valencia, S. Gompers, and Y. Shih, "Remote spectral measurement using entangled photons," *Appl. Phys. Lett.*, vol. 83, no. 26, pp. 5560–5562, 2003.

[14] P. Janassek, S. Blumenstein, and W. Elsäßer, "Ghost spectroscopy with classical thermal light emitted by a superluminescent diode," *Phys. Rev. Appl.*, vol. 9, no. 2, 2018, Art. no. 021001.

[15] C. Amiot, P. Ryczkowski, A. T. Friberg, J. M. Dudley, and G. Genty, "Supercontinuum spectral-domain ghost imaging," *Opt. Lett.*, vol. 43, no. 20, pp. 5025–5028, 2018.

[16] O. Smirnova *et al.*, "High harmonic interferometry of multi-electron dynamics in molecules," *Nature*, vol. 460, no. 7258, pp. 972–977, 2009.

[17] C. Voisin, N. Del Fatti, D. Christofilos, and F. Vallée, "Ultrafast electron dynamics and optical nonlinearities in metal nanoparticles," *J. Phys. Chem. B*, vol. 105, no. 12, pp. 2264–2280, 2001.

[18] Y. B. Band, *Light and Matter: Electromagnetism, Optics, Spectroscopy and Lasers*, vol. 1. Hoboken, NJ, USA: Wiley, 2006.

[19] L. V. Wang and H.-i. Wu, *Biomedical Optics: Principles and Imaging*. Hoboken, NJ, USA: Wiley, 2012.

[20] A. Klein, I. Sibony, S. Meir, H. Duadi, M. Y. Sander, and M. Fridman, "Temporal imaging with a high filling factor," *APL Photon.*, vol. 5, no. 9, 2020, Art. no. 090801.

[21] S. Asraf, M. Fridman, and Z. Zalevsky, "Fibers-based temporal super-resolved imaging," *Sci. Rep.*, vol. 10, no. 1, pp. 1–11, 2020.

[22] A. Klein, I. Sibony, S. Meir, S. Shahal, H. Duadi, and M. Fridman, "Overlapping time-lens array," *IEEE Photon. J.*, vol. 11, no. 3, Jun. 2019, Art. no. 3200106.

[23] H. Duadi, T. Yaron, A. Klein, S. Meir, and M. Fridman, "Phase retrieval by an array of overlapping time-lenses," *Opt. Lett.*, vol. 44, no. 4, pp. 799–802, 2019.

[24] I. Del Villar, O. Fuentes, F. Chiavaioli, J. M. Corres, and I. R. Matias, "Optimized strain long-period fiber grating (LPFG) sensors operating at the dispersion turning point," *J. Lightw. Technol.*, vol. 36, no. 11, pp. 2240–2247, 2018.

[25] F. Chiavaioli, F. Baldini, and C. Trono, "Manufacturing and spectral features of different types of long period fiber gratings: Phase-shifted, turn-around point, internally tilted, and pseudo-random," *Fibers*, vol. 5, no. 3, p. 29, 2017.

[26] J. W. Goodman, *Statistical Optics*. Hoboken, NJ, USA: Wiley, 2015.

[27] J. García, Z. Zalevsky, and D. Fixler, "Synthetic aperture superresolution by speckle pattern projection," *Opt. Exp.*, vol. 13, no. 16, pp. 6073–6078, 2005.

[28] J. C. Dainty, *Laser Speckle and Related Phenomena*, vol. 9. Berlin, Germany: Springer, 2013.